Standardized Matrix Modeling of Multiple Energy Systems

Yi Wang, *Student Member, IEEE*, Ning Zhang, *Member, IEEE*, Chongqing Kang, *Fellow, IEEE*, Daniel S. Kirschen, *Fellow, IEEE*, Jingwei Yang, *Student Member, IEEE*, and Qing Xia, *Senior Member, IEEE*

***Abstract*—Multiple energy systems (MESs) bring together the electric power, heat, natural gas, and other systems to improve the overall efficiency of the energy system. An energy hub (EH) models an MES as a device with multiple ports using a matrix coupling the inputs and outputs. This paper proposes a standardized matrix modeling method based on the concept of EH to build the coupling matrix automatically. The components and the structure of MES are first defined using graph theory. Then, the matrices describing the topology of the MES and the characteristics of the energy converters are developed. On this basis, the energy flow equations are formulated. Gaussian elimination can then be applied to obtain the coupling matrix and analyze the degree of freedom of the EH. A standard data structure for basic information on the MES is proposed to facilitate computerized modeling. Further, extension modeling of energy storage and demand response is also discussed. Finally, a case study of a modified tri-generation system is conducted to illustrate the proposed method.**

***Index Terms*—Multiple energy systems, energy hub, coupling matrix, matrix modeling, operation optimization.**

NOMENCLATURE

Indices

b	Index of branches. $b = 1 \cdots B$.
f	Degree of freedom of the EH.
g	Index of nodes. $g = 1 \cdots G$.
k	Index of ports. $k = 1 \cdots K$.
m	Number of output ports.
n	Number of input ports.

Vectors and Matrices

$\boldsymbol{A}_g$	Port-branch incidence matrix.
$\boldsymbol{A}_g'$	Augmented port-branch incidence matrix.
$\boldsymbol{C}$	Coupling matrix of EH.
$\boldsymbol{E}$	Energy stored in storages.
$\boldsymbol{E}_{\min}$	Minimum energy stored in storages.
$\boldsymbol{E}_{\max}$	Maximum energy stored in storages.
$\Delta\boldsymbol{E}$	Changes of energy stored in storages.
$\boldsymbol{H}_g$	Converter characteristic matrix.
$\boldsymbol{M}_{g,k}$	Port-branch incidence vector.
$\boldsymbol{V}$	Branch set.
$\boldsymbol{V}_{in}$	Energy input vector of EH.
$\boldsymbol{V}_{out}$	Energy output vector of EH.
$\boldsymbol{X}$	Input incidence matrix.
$\boldsymbol{Y}$	Output incidence matrix.
$\boldsymbol{Z}$	System energy conversion matrix.
$\boldsymbol{Z}_g$	Nodal energy conversion matrix.

Manuscript received December 11, 2016; revised April 27, 2017 and June 21, 2017; accepted August 5, 2017. Date of publication August 9, 2017; date of current version December 19, 2018. This work was supported by the National Science Foundation of China under Grant 51620105007 and Grant 51677096. Paper no. TSG-01743-2016. *(Corresponding author: Chongqing Kang.)*

Y. Wang, N. Zhang, C. Kang, J. Yang, and Q. Xia are with the State Key Laboratory of Power Systems, Department of Electrical Engineering, Tsinghua University, Beijing 100084, China (e-mail: cqkang@tsinghua.edu.cn).

D. S. Kirschen is with the Department of Electrical Engineering, University of Washington, Seattle, WA 98195-2500 USA.

Color versions of one or more of the figures in this paper are available online at http://ieeexplore.ieee.org.

Digital Object Identifier 10.1109/TSG.2017.2737662

I. INTRODUCTION

INTEGRATING the generation, transmission, storage and consumption of electricity, heat, cooling and gas in multiple energy systems (MES) is an effective way to improve overall energy efficiency and to facilitate the integration of large amounts of renewable energy. MES has therefore been the subject of a large number of theoretical and practical research projects in recent years [1].

As MES become large and more complex, the need arises for a systematic and automated method to generate models that can be used for optimizing the operation and the planning of these systems. This paper proposes such a method. In particular, it presents a standardized formulation of the coupling matrix of the energy hub (EH), which forms the heart of the MES.

An MES consists of devices that convert energy from one form to another using various technologies. Examples of such converters include combined cooling, heat, and power (CCHP) units, combined heat and power (CHP) units, power to gas (P2G) equipment, electric boilers, heat pumps, gas-fired boilers, and absorption refrigeration units [2]. Modeling the conversion and coupling relationship of is challenging because of the large number of possible combinations of devices and topologies.

In 2007, Geidl *et al.* [3] put forward the concept of EH. An EH is a universal MES component that can convert, condition, and store different forms of energy. An EH has multiple input and output ports and creates an interface between different energy carriers. Each EH is modeled by a coupling matrix that defines the distribution, conversion and coupling

relationships between the energy inputs and outputs. The compactness and effectiveness of the EH-based modeling facilitate the calculation of energy flows in MES, as well as the optimization of their operation and planning [4]. Since then, the concept of coupling matrix has been expanded to include demand response [5], [6], storage [7], [8], electrical vehicles (EV) [9], [10], and renewable energy sources [11]. Optimizing the operation of EH can involve a single EH or the coordinated optimization of multiple EHs [12]. It can focus on residential consumers [13], commercial buildings [14], and cross-regional MES [15]. Optimal planning of EH addresses the questions of whether, when and where to invest in energy converters and what size they should have to achieve the best economic or environmental benefits [16], [17].

While a substantial number of papers discuss the optimal operation and planning of EH, very few papers study the automatic modeling of it. Chicco and Mancarella [18] have proposed a technique to generate automatically coupling matrices for small-scale tri-generation systems. However, dispatch factors are usually used to model interconnected systems. The formulation involves products of decision variables and leads to nonlinear rather than linear optimization problems. The path searching used for matrix modeling method is too complex for large MES and involves symbolic computation that is hard to be automated. Almassalkhi and Towle [19] propose a linear modeling method for EH with an energy "input-storage-conversion-storage-output" structure. The nonlinearity brought by non-constant efficiencies is addressed by piecewise linear approximations. However, this model can only deal with the proposed structure of MES where the location of components such as energy storages are fixed. It is significant for a modeling method to be applicable to a wide variety of MES and is able to be implemented by a computer. More flexible and automatic modeling method is needed.

The standardized matrix modeling method proposed in this paper deals with the nonlinear problem from dispatch factors by using the energy flow between the converters as the state variables. Since the relationship between any two energy flows is linear, there is no need to introduce dispatch factors as decision variables. Then, the proposed method uses graph theory to cast the topology and the characteristics of the energy converters into matrix form. The equations of the EH then describe the energy balance in each energy converter. Finally, the coupling matrix is obtained through Gaussian elimination.

This paper makes the following original contributions:

1) It proposes a standardized matrix modeling method for MES including energy storage and integrated demand response that can be easily and compactly automated.
2) The proposed method reduces the nonlinearity of EH model, which makes the solution of optimization problems significantly easier than compared to the use of dispatch factors embedded in the coupling matrix.
3) This approach provides a way to comprehensively analyze the inherent flexibility of the EH according to the degree of freedom of the linearized formulation.

The remainder of the paper is organized as follows. Section II describes the standardized MES model. Section III shows how the EH coupling matrix can be calculated using Gaussian elimination and analyzes the degree of freedom of the EH. Section IV extends the model to energy storage and integrated demand response. Section V defines the standardized data structure for the computer-aided analysis of MES. Section VI illustrates the proposed method using the tri-generation system as a case study. Section VII draws conclusions.

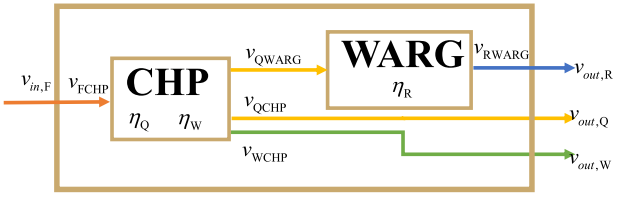

Fig. 1. A CCHP-based MES.

II. Standardized Modeling Method

A. EH Concept

An EH models an MES of any complexity as a unit with multiple input and output ports. The energy injected into the input ports, in the form of gas, electricity, heat or other vectors, are described by a vector $\boldsymbol{V}_{in}$ of dimension m. Similarly, the energy outputs are described by a vector $\boldsymbol{V}_{out}$ of dimension n. The **coupling matrix** $\boldsymbol{C}$ defines the steady-state relationship between $\boldsymbol{V}_{in}$ and $\boldsymbol{V}_{out}$ at a certain period.

$$\boldsymbol{V}_{in} = \boldsymbol{C}\boldsymbol{V}_{out} \tag{1}$$

Figure 1 shows a CCHP-based MES which consists of a CHP unit and a water absorption refrigerator group (WARG). This simple example is used here to illustrate how to formulate an EH model and, in later sections, the development of the proposed standardized matrix modeling method.

The sole energy input of this CCHP system is natural gas $v_{in,\mathrm{F}}$. The CHP unit uses natural gas to produce electricity with efficiency η_{W} and heat with efficiency η_{Q}. The CHP is assumed to operate in back pressure mode except in special circumstances. The electricity produced by the CHP (v_{WCHP}) goes directly to the $v_{out,\mathrm{W}}$ output of the EH. On the other hand, its heat output is divided into three parts: direct supply ($v_{out,\mathrm{Q}}$) and input to the WARG (v_{QWARG}). The WARG converts its heat input into cooling (v_{RWARG}) for supply ($v_{out,\mathrm{R}}$) with an efficiency of η_{R}. The input and output vectors of the EH model of this CCHP-based MES are:

$$\begin{aligned} \boldsymbol{V}_{in} &= \begin{bmatrix} v_{in,\mathrm{F}} \end{bmatrix} \\ \boldsymbol{V}_{out} &= \begin{bmatrix} v_{out,\mathrm{R}} & v_{out,\mathrm{Q}} & v_{out,\mathrm{W}} \end{bmatrix}^T \end{aligned} \tag{2}$$

The coupling matrix $\boldsymbol{C}$ is a 1x3 vector that can be written directly using energy dispatch and efficiency factors:

$$\boldsymbol{C} = \begin{bmatrix} \eta_{\mathrm{Q}}\alpha_{\mathrm{R}}\eta_{\mathrm{R}} & \eta_{\mathrm{Q}}\alpha_{\mathrm{Q}} & \eta_{\mathrm{W}} \end{bmatrix}^T \tag{3}$$

where the dispatch factors α_{Q} and α_{R} reflect the proportions of the heat energy that is supplied and used for refrigeration.

When optimizing the operation of the EH, the natural gas input $v_{in,\mathrm{F}}$ and the dispatch factors α_{Q} and α_{R} are decision variables while (3) is a constraint. Since this constraint

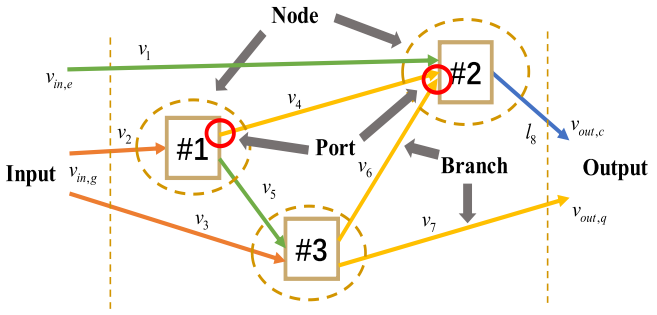

Fig. 2. Definitions of basic element of an EH in terms of graph theory.

involves two products of decision variables ($v_{in,\mathrm{F}}\alpha_{\mathrm{Q}}$ and $v_{in,\mathrm{F}}\alpha_{\mathrm{R}}$), this optimization problem is nonlinear and thus difficult to solve. In this case the coupling matrix $\boldsymbol{C}$ could be formulated easily. However, in more complex systems, building this matrix requires an exhaustive manual description of the energy flows and symbolic matrix manipulations.

A MES typically includes several energy converters and their topology can be quite complex. Streamlining the modeling of the energy conversion, storage, and distribution processes that take place in an MES is, therefore, a key issue.

B. Basic Definitions in EH

Modeling an MES requires modeling the energy conversion devices that it comprises and their connections. This section describes a standardized matrix modeling based on graph theory, where the characteristics of energy converters and their topology are expressed in matrix form. Figure 2 shows the connections between the three energy converters (#1, #2, and #3) of a simple illustrative MES.

Each energy converter in an EH can be treated as a node in a graph. Energy hubs can then be analyzed using graph theory [20] if we link their physical components to graph theory concepts as follows:

- Each energy flow to or from a converter is represented by a *branch*. Branches, therefore, carry energy flows in any vector (e.g., gas, electricity, heat, cooling)
- A *node* is the abstraction of an energy converter and also the abstraction of the branch endpoints. Inputs and outputs are treated as special nodes
- Each node has one or more *ports* through which it exchanges energy with other nodes. Each converter has a fixed number of input and output ports. For example, a CHP unit has one input port for gas and two output ports for electricity and heat.
- A *graph* is a collection of nodes and branches.
- An EH is an *oriented graph* because each branch has a specified direction, i.e., from a source to a sink.

Note that these definitions of nodes and branches in EH are different from those used in power system analysis.

C. Port-Branch Incidence Vectors and Matrices

A *port-branch incidence vector* defines the connections between the ports of a node and the branches. Let us consider an EH with G nodes (energy converters) and B branches (energy flows). The *port-branch incidence vector* $\boldsymbol{M}_{g,k}$ of port k of the node g is a vector of dimension B, which defines the connections between this port and all the branches. The elements of $\boldsymbol{M}_{g,k}$ are:

$$m_b = \begin{cases} 1 & \text{branch } b \text{ is connected to input port } k \text{ of node } g \\ -1 & \text{branch } b \text{ is connected to output port } k \text{ of node } g \\ 0 & \text{branch } b \text{ is not connected to any port of node } g \end{cases} \tag{4}$$

Note that each port can be connected to multiple branches. If the *node* g has K_g ports, the *port-branch incidence matrix* $\boldsymbol{A}_g$ of node g has dimensions K_g x B and is defined as follows:

$$\boldsymbol{A}_g = \left[\boldsymbol{M}_{g,1}, \boldsymbol{M}_{g,2}, \ldots, \boldsymbol{M}_{g,K_g}\right]^T \tag{5}$$

The port-branch incidence matrix of a node thus contains all the information about the connections between this node and all the branches. In the example of Fig. 2, if we assume that the CHP unit is Node #1 and the WARG Node #2, the set of branches (energy flows) can be written as:

$$\boldsymbol{V} = \left[v_{\mathrm{FCHP}} \;\; v_{\mathrm{QWARG}} \;\; v_{\mathrm{QCHP}} \;\; v_{\mathrm{WCHP}} \;\; v_{\mathrm{RWARG}}\right]^T \tag{6}$$

If the natural gas input port of the CHP unit is labeled 1, while its heat and electricity output ports are numbered 2, and 3 respectively, the port-branch incidence matrix of this node is:

$$\boldsymbol{A}_{1,3\times 5} = \begin{bmatrix} 1 & 0 & 0 & 0 & 0 \\ 0 & -1 & -1 & 0 & 0 \\ 0 & 0 & 0 & -1 & 0 \end{bmatrix}. \tag{7}$$

D. Converter Characteristic Matrices

The *converter characteristic matrix* $\boldsymbol{H}_g$ of node g defines the energy conversion characteristics of the node. It has as many rows as there are energy conversion processes and as many columns as there are input and output ports. The columns are ranked by port number. Depending on the characteristics of the converter, there are four types.

1) Type 1 (Single Input Port and Single Output Port): This type of converters includes electric boilers, air conditioners, and absorption refrigeration units. Since there is only one energy conversion process, the energy output is proportional to the input. Since there are two ports, matrix $\boldsymbol{H}_g$ is of dimension 1×2. The η_g denotes the efficiency of converter g is linked to the input port and a "1" to the output port:

$$\boldsymbol{H}_g = \begin{bmatrix} \eta_g & 1 \end{bmatrix} \tag{8}$$

For example, the converter characteristic matrix of the WARG in Fig. 1 is:

$$\boldsymbol{H}_2 = \begin{bmatrix} \eta_R & 1 \end{bmatrix}. \tag{9}$$

2) Type 2 (Single Input Port and Multiple Output Ports): If the energy output of each output port is proportional to the energy input, the number of rows is equal to the number of output ports. The elements of $\boldsymbol{H}_g$ for the row corresponding to output port i are then:

$$h_{i,k} = \begin{cases} \eta_i \text{ if } k \text{ is the number of the input port} \\ 1 \text{ if } k \text{ is the number of the output port } i \\ 0 \text{ otherwise} \end{cases} \tag{10}$$

where, η_i is the efficiency of the energy conversion process from the input port to output port i. For example, if the CHP unit in Fig. 2 is in back pressure operation, the production of electricity and heat are both proportional to the gas input. Matrix $\boldsymbol{H}_g$ is then:

$$\boldsymbol{H}_1 = \begin{bmatrix} \eta_{\mathrm{Q}} & 1 & 0 \\ \eta_{\mathrm{W}} & 0 & 1 \end{bmatrix} \tag{11}$$

If the proportion of energy directed to output port can be flexibly adjusted, $\boldsymbol{H}_g$ has only one row and can be built using the energy balance of the converter:

$$h_{1,k} = \begin{cases} 1 & \text{if } k \text{ is the number of input port} \\ 1/\eta_i & \text{if } k \text{ is the number of output port } i \end{cases} \tag{12}$$

A CHP unit in extraction condensing operation mode is an example of such a component because the ratio between electricity and heat production is adjustable within a certain range. The matrix $\boldsymbol{H}_g$ then has one row and three columns:

$$\boldsymbol{H}_1 = \begin{bmatrix} 1 & 1/\eta_{\mathrm{Q}} & 1/\eta_{\mathrm{W}} \end{bmatrix}. \tag{13}$$

3) Type 3 (Multiple Input Ports and Single Output Port): If the energy input through each input port is proportional to the energy output, the converter characteristic MATRIX is similar to those of *Type* 1. Each input port corresponds to one row of $\boldsymbol{H}_g$. The elements of the row corresponding to input port i are then

$$h_{i,k} = \begin{cases} \eta_i & \text{if } k \text{ is the number of input port } i \\ 1 & \text{if } k \text{ is the number of output port} \\ 0 & \text{elsewise} \end{cases} \tag{14}$$

If the proportion of energy inputs of multiple input ports can be adjusted, $\boldsymbol{H}_g$ is a single row matrix where the terms can be calculated using the energy balance of the converter:

$$h_{1,k} = \begin{cases} \eta_i & \text{if } k \text{ is the number of input port } i \\ 1 & \text{if } k \text{ is the number of output port.} \end{cases} \tag{15}$$

4) Type 4 (Multiple Input Ports and Multiple Output Ports): If the energy inputs (outputs) are proportional to the energy output (inputs), $\boldsymbol{H}_g$ can be formulated according to Eq. (10) (Eq. (14)). Otherwise, $\boldsymbol{H}_g$ can be formulated according to Eq. (12) (Eq. (15)).

The energy conversion matrices $\boldsymbol{H}_g$ are determined solely by the characteristics of the converters, irrespective of the topology of EH. For a given type of converter in a given operation mode, the energy conversion matrix is fixed. Since the number of converter types in basic MES is limited, these matrices can be formulated beforehand, which simplifies the standardized matrix modeling and computerized analysis.

E. Energy Conversion Matrices

Given the port-branch incidence matrix and the converter characteristic matrix, we can calculate the *nodal energy conversion matrix* for node g:

$$\boldsymbol{Z}_g = \boldsymbol{H}_g \boldsymbol{A}_g \tag{16}$$

This matrix combines the energy converter characteristics and the connections between node g and all branches. The nodal energy conversion matrix of the CHP unit of Fig. 2 is:

$$\boldsymbol{Z}_1 = \begin{bmatrix} \eta_{\mathrm{Q}} & -1 & -1 & 0 & 0 \\ \eta_{\mathrm{W}} & 0 & 0 & -1 & 0 \end{bmatrix} \tag{17}$$

The *system energy conversion matrix* $\boldsymbol{Z}$ combines the nodal energy conversion matrix of all nodes in the EH:

$$\boldsymbol{Z} = \begin{bmatrix} \boldsymbol{Z}_1^T & \boldsymbol{Z}_2^T & \cdots & \boldsymbol{Z}_N^T \end{bmatrix}^T \tag{18}$$

The system energy conversion matrix is similar to the node-branch incidence matrix in power network analysis because both of them describe the relationship between nodes and branches. The only difference is that the former takes into account the conversion characteristics or efficiencies. For the MES of Fig. 2, the system energy conversion matrix $\boldsymbol{Z}$ is:

$$\boldsymbol{Z} = \begin{bmatrix} \eta_{\mathrm{Q}} & -1 & -1 & 0 & 0 \\ \eta_{\mathrm{W}} & 0 & 0 & -1 & 0 \\ 0 & \eta_{\mathrm{R}} & 0 & 0 & -1 \end{bmatrix}. \tag{19}$$

F. Comprehensive Energy Flow Equations for EH

Let v_b be the energy flow in branch b. The energy flows in all branches form a $B \times 1$ vector $\boldsymbol{V}$. According to the energy conversion characteristic of each node, we can obtain the *energy conversion equation* of the EH:

$$\boldsymbol{ZV} = \boldsymbol{0} \tag{20}$$

We define the m-dimensional energy input vector $\boldsymbol{V}_{in}$ and the n-dimensional energy output vector $\boldsymbol{V}_{out}$. The *input incidence matrix* $\boldsymbol{X}$ is a $n \times B$ matrix that relates the energy inputs to the branch energy flows. Similarly, the *output incidence matrix* $\boldsymbol{Y}$ is a $m \times B$ matrix that relates the energy outputs to the branch energy flows:

$$x_{ib} = \begin{cases} 1 & \text{if input node } i \text{ is source of branch } b \\ 0 & \text{otherwise} \end{cases} \tag{21}$$

$$y_{ib} = \begin{cases} 1 & \text{if output node } i \text{ is sink of branch } b \\ 0 & \text{otherwise} \end{cases} \tag{22}$$

The input incidence and output incidence equations are:

$$\boldsymbol{V_{in}} = \boldsymbol{XV} \tag{23}$$

$$\boldsymbol{V_{out}} = \boldsymbol{YV} \tag{24}$$

While (20) describes the energy coupling within the EH, (23) and (24) describe the external coupling. Together, these three equations form the *comprehensive energy flow equations* of the EH:

$$\begin{bmatrix} \boldsymbol{X} \\ \boldsymbol{Y} \\ \boldsymbol{Z} \end{bmatrix} \boldsymbol{V} = \begin{bmatrix} \boldsymbol{V}_{in} \\ \boldsymbol{V}_{out} \\ \boldsymbol{0} \end{bmatrix} \tag{25}$$

Taking the CCHP system of Fig. 2 as an example, the input incidence matrix is:

$$\boldsymbol{X} = \begin{bmatrix} 1 & 0 & 0 & 0 & 0 \end{bmatrix} \tag{26}$$

The output incidence matrix is:

$$\boldsymbol{Y} = \begin{bmatrix} 0 & 0 & 0 & 0 & 1 \\ 0 & 0 & 1 & 0 & 0 \\ 0 & 0 & 0 & 1 & 0 \end{bmatrix} \tag{27}$$

The comprehensive equation of this EH are then:

$$\begin{bmatrix} 1 & 0 & 0 & 0 & 0 \\ 0 & 0 & 0 & 0 & 1 \\ 0 & 0 & 1 & 0 & 0 \\ 0 & 0 & 0 & 1 & 0 \\ \eta_{\mathrm{Q}} & -1 & -1 & 0 & 0 \\ \eta_{\mathrm{W}} & 0 & 0 & -1 & 0 \\ 0 & \eta_{\mathrm{R}} & 0 & 0 & -1 \end{bmatrix} \begin{bmatrix} v_{\mathrm{FCHP}} \\ v_{\mathrm{QWARG}} \\ v_{\mathrm{QCHP}} \\ v_{\mathrm{WCHP}} \\ v_{\mathrm{RWARG}} \end{bmatrix} = \begin{bmatrix} v_{in,\mathrm{F}} \\ v_{out.\mathrm{W}} \\ v_{out.\mathrm{Q}} \\ v_{out.\mathrm{R}} \\ 0 \\ 0 \\ 0 \end{bmatrix} \tag{28}$$

Note that the efficiencies η_{W}, η_{Q}, and η_{R} in the model could be a function of the load or time, and this would make the model nonlinear. Several techniques such as piecewise linear approximations can be used to deal with these non-linearities [19].

III. Calculation of the Coupling Matrix Using Gaussian Elimination

In the comprehensive power flow equations, the energy conversion equation acts as a bridge between the input vector $\boldsymbol{V}_{in}$ and the output vector $\boldsymbol{V}_{out}$. A direct relation between $\boldsymbol{V}_{in}$ and $\boldsymbol{V}_{out}$, i.e., a coupling matrix, can be obtained through Gaussian elimination. Moving the input vector $\boldsymbol{V}_{in}$ to the left-hand side of the equations while keeping the output vector $\boldsymbol{V}_{out}$ on the right-hand side, we get:

$$\begin{bmatrix} \boldsymbol{0} & \boldsymbol{Y} \\ -\boldsymbol{I} & \boldsymbol{X} \\ \boldsymbol{0} & \boldsymbol{Z} \end{bmatrix} \begin{bmatrix} \boldsymbol{V}_{in} \\ \boldsymbol{V} \end{bmatrix} = \begin{bmatrix} \boldsymbol{V}_{out} \\ \boldsymbol{0} \\ \boldsymbol{0} \end{bmatrix} \tag{29}$$

Separating the second and third row blocks of (29):

$$\begin{bmatrix} -\boldsymbol{I} \\ \boldsymbol{0} \end{bmatrix} \boldsymbol{V}_{in} + \begin{bmatrix} \boldsymbol{X} \\ \boldsymbol{Z} \end{bmatrix} \boldsymbol{V} = \boldsymbol{0} \tag{30}$$

Labeling the matrices $\begin{bmatrix} -\boldsymbol{I} \\ \boldsymbol{0} \end{bmatrix}$ and $\begin{bmatrix} \boldsymbol{X} \\ \boldsymbol{Z} \end{bmatrix}$ respectively $\boldsymbol{R}$ and $\boldsymbol{Q}$, we have:

$$\boldsymbol{R}\boldsymbol{V}_{in} + \boldsymbol{Q}\boldsymbol{V} = \boldsymbol{0} \tag{31}$$

If matrix $\boldsymbol{Q}$ is invertible, we can express the branch energy flow vector $\boldsymbol{V}$ in terms of the input vector $\boldsymbol{V}_{in}$, and substitute it into (24) to obtain the relation between $\boldsymbol{V}_{in}$ to $\boldsymbol{V}_{out}$. Whether this is possible depends on the dimensions and rank of $\boldsymbol{Q}$, which are determined by the characteristics of the energy converters and their connections. As we saw in the previous section, there are four types of energy converters: 1) single input/single output; 2) single input/multiple outputs; 3) multiple inputs/single output; 4) multiple inputs/multiple outputs. Furthermore, each input port of node (or output of the overall EH) can be connected either 1) to a single branch, or 2) to multiple branches. Similarly, each output port of node (or input of the overall EH) can be connected either 1) to a single branch or 2) to multiple branches. The dimensions of $\boldsymbol{Q}$ are thus a function of the types of energy converters, of the input ports connection and of the output port connections. We denote each case by a triplet shown in the brackets. For example, 1-1-1 means a converter with a single input and a single output where the input port connects with only one branch and the output port connects with only one branch. Let us assume that the total number of energy conversion equations is θ, the number of branches that are connected to the overall input of the EH is μ, and the total number of output ports of all of the nodes in the EH is λ. Matrix $\boldsymbol{X}$ is then of dimension $\mu \times B$, matrix $\boldsymbol{Z}$ of dimension $\theta \times B$, and matrix $\boldsymbol{Q}$ of dimension $(\mu + \theta) \times B$.

Case A (1-1-1, 1-2-1): Since each output port connects with only one branch and each output corresponds to one energy conversion equation ($\lambda = \theta$), each branch is either connected to an output or overall input of the EH. Therefore $\mu + \lambda = B$, $\mu + \theta = \mu + \lambda = B$, and $\boldsymbol{Q}$ is a $B \times B$ full rank matrix. We can then write:

$$\boldsymbol{V} = -\boldsymbol{Q}^{-1}\boldsymbol{R}\boldsymbol{V}_{in} \tag{32}$$

Substituting (32) into (24), we get:

$$\boldsymbol{V}_{out} = -\boldsymbol{Y}\boldsymbol{Q}^{-1}\boldsymbol{R}\boldsymbol{V}_{in} \tag{33}$$

The coupling matrix $\boldsymbol{C}$ is then:

$$\boldsymbol{C} = -\boldsymbol{Y}\boldsymbol{Q}^{-1}\boldsymbol{R}. \tag{34}$$

Case B (2-1-1, 2-2-1): As in Case A, we still have $\mu + \lambda = B$. We must consider two sub-cases:

1) Each output port corresponds to one energy conversion equation. We then have $\lambda = \theta$, and $\mu + \theta = \mu + \lambda = B$. $\boldsymbol{Q}$ is then again a $B \times B$ full rank matrix and $\boldsymbol{C}$ can be calculated as in (34).

2) There are fewer energy conversion equations than the number of the output port. Therefore $\theta < \lambda$ as illustrated by (14). The dimensions of matrix $\boldsymbol{Q}$ are then $(B - \lambda + \theta) \times B$ and (31) is underdetermined with a degree of freedom of $(\lambda - \theta)$. We partition matrix $\boldsymbol{Q}$ into two blocks $[\boldsymbol{Q}_1 \quad \boldsymbol{Q}_2]$ in such a way that $\boldsymbol{Q}_1$ is a $(B - \lambda + \theta) \times (B - \lambda + \theta)$ full rank matrix. If we partition $\boldsymbol{V}$ and $\boldsymbol{Y}$ in the same way as $\boldsymbol{Q}$, Eqs. (31) and (24) can be rewritten as:

$$\boldsymbol{R}\boldsymbol{V}_{in} + \begin{bmatrix} \boldsymbol{Q}_1 & \boldsymbol{Q}_2 \end{bmatrix} \begin{bmatrix} \boldsymbol{V}_1 \\ \boldsymbol{V}_2 \end{bmatrix} = \boldsymbol{0} \tag{35}$$

$$\boldsymbol{V}_{out} = \begin{bmatrix} \boldsymbol{Y}_1 & \boldsymbol{Y}_2 \end{bmatrix} \begin{bmatrix} \boldsymbol{V}_1 \\ \boldsymbol{V}_2 \end{bmatrix} \tag{36}$$

Combining Eq. (35) and (36), we get:

$$\boldsymbol{V}_{out} = \begin{bmatrix} -\boldsymbol{Y}_1\boldsymbol{Q}_1^{-1}\boldsymbol{R} & \boldsymbol{Y}_2 - \boldsymbol{Y}_1\boldsymbol{Q}_1^{-1}\boldsymbol{Q}_2 \end{bmatrix} \begin{bmatrix} \boldsymbol{V}_{in} \\ \boldsymbol{V}_2 \end{bmatrix} \tag{37}$$

If the subset of branch flows $\boldsymbol{V}_2$ is defined as a set of state variables, the EH model is linear without dispatch factors. Then, we can define the generalized coupling matrix $\boldsymbol{C}'$:

$$\boldsymbol{C}' = \begin{bmatrix} -\boldsymbol{Y}_1\boldsymbol{Q}_1^{-1}\boldsymbol{R} & \boldsymbol{Y}_2 - \boldsymbol{Y}_1\boldsymbol{Q}_1^{-1}\boldsymbol{Q}_2 \end{bmatrix} \tag{38}$$

Note that choosing a different set of branch flows as state variables leads to a different matrix $\boldsymbol{C}'$.

Case C (3-1-1, 3-2-1): If each output port corresponds to one energy conversion equation, we have $\theta = \lambda$, and, as in *Case A*, $\boldsymbol{Q}$ is a $B \times B$ full rank matrix. If there is more than one energy conversion equation for some converters (i.e., $\theta > \lambda$), the dimensions of $\boldsymbol{Q}$ are $(B - \lambda + \theta) \times B$. Equation (31) is then over-determined and may not have a solution. In such a case, the model is unreasonable or the modeled system is physically

TABLE I
DEGREE OF FREEDOM OF THE EH UNDER DIFFERENT CONDITIONS

Output port type / Energy converters type	Each of the output port connects to a single branch	Some of the output port connect to multiple branches
Single input / single output	$\boldsymbol{Q}$ is a $B\times B$ full rank matrix. Degree of freedom is zero.	$\boldsymbol{Q}$ is a $(B-\tau)\times B$ matrix. Degree of freedom is τ .
Single input/multiple outputs	$\boldsymbol{Q}$ is a $(B-\lambda+\theta)\times B$ matrix. Degree of freedom is $\lambda-\theta$.	$\boldsymbol{Q}$ is a $(B-\lambda+\theta-\tau)\times B$ matrix. Degree of freedom is $\lambda-\theta+\tau$.
Multiple inputs/single output		
Multiple inputs/ multiple outputs		

infeasible, additional flexibility needs to be introduced in the model or in the practical system.

Case D (4-1-1, 4-2-1): This is a combination of *Case B* and *Case C*. $\boldsymbol{Q}$ is of dimension $(B-\lambda+\theta)\times B$. Whether (31) is determined, under-determined or over-determined depends on the values of θ and λ.

Case E (1-1-2, 1-2-2): As in *Case A*, we have $\theta=\lambda$. If τ is the total number of extra branches that connect to each port (e.g., if the output port is connected with 2 branches, $\tau=1$; if the output port is connected with 3 branches, $\tau=2$; and so on), we have $\theta=B-\mu-\tau$ and $\boldsymbol{Q}$ is of dimension $(B-\tau)\times B$. Equation (31) is under-determined and can be handled like (37), with τ degrees of freedom.

Case F (4-2-2): Based on the analysis for *Case D* and *Case E*, we can conclude that $\boldsymbol{Q}$ is of dimension $(B-\lambda+\theta-\tau)\times B$. Cases *A* to *E* above can all be viewed as special cases of *Case F*. The degree of freedom of the EH is:

$$f=\lambda-\theta+\tau \tag{39}$$

where the values of λ and θ are related to the characteristic of the energy converters, while τ is determined by the connections between the ports and the branches, which corresponds to the number of dispatch factors. Thus, the degree of freedom of the whole EH is a combination of the inherent flexibility of the converters and the external connection topology. However, if some of the columns of $\boldsymbol{Q}_2$ are not linearly independent, the degree of freedom of the system will be reduced.

The cases analyzed above can be summarized in Table I.

Taking the example of Fig. 2, the $\boldsymbol{Q}$ matrix of the EH is:

$$\boldsymbol{Q}=\begin{bmatrix}1&0&0&0&0\\ \eta_{\mathrm{Q}}&-1&-1&0&0\\ \eta_{\mathrm{W}}&0&0&-1&0\\ 0&\eta_{\mathrm{R}}&0&0&-1\end{bmatrix} \tag{40}$$

The rank of $\boldsymbol{Q}$ is four and the degree of freedom of (31) is one. Physically, this stems from the fact that we can choose how to dispatch between v_{QWARG} and $v_{out,\mathrm{Q}}$. If we select the flow on branch v_{QWARG} as a state variable, the output vector $\boldsymbol{v}_{out}$ can be formulated as:

$$\boldsymbol{V}_{out}=\begin{bmatrix}0\\ \eta_{Q}\\ \eta_{\mathrm{W}}\end{bmatrix}\boldsymbol{V}_{in}+\begin{bmatrix}\eta_{\mathrm{R}}\\ -1\\ 0\end{bmatrix}v_{QWARG} \tag{41}$$

On the other hand, if the CHP unit in Fig. 2 works in extraction condensing operation mode, we have:

$$\boldsymbol{Q}=\begin{bmatrix}1&0&0&0&0\\ 1&-1/\eta_{\mathrm{Q}}&-1/\eta_{\mathrm{Q}}&1/\eta_{\mathrm{W}}&0\\ 0&\eta_{\mathrm{R}}&0&0&-1\end{bmatrix} \tag{42}$$

The rank of $\boldsymbol{Q}$ is then three and the degree of freedom of (31) is two. This additional degree of freedom compared with back pressure operation stems from the flexibility between electric and heat output of the CHP unit in this operating mode.

Using the method described above, we can obtain the dispatch factor embedded in the coupling matrix. The dispatch between v_{QWARG} and $v_{out,\mathrm{Q}}$ can be modeled as a constraint $v_{QWARG}/v_{out,Q}=\alpha_{\mathrm{Q}}/\alpha_{\mathrm{R}}$. Adding this constraint to the matrix $\boldsymbol{Z}$, we have:

$$\boldsymbol{Z}=\begin{bmatrix}\eta_{\mathrm{Q}}&-1&-1&0&0\\ \eta_{\mathrm{W}}&0&0&-1&0\\ 0&\eta_{\mathrm{R}}&0&0&-1\\ 0&-\alpha_{\mathrm{Q}}&\alpha_{\mathrm{R}}&0&0\end{bmatrix} \tag{43}$$

$\boldsymbol{Q}$ is then a full rank matrix. According to (34), the coupling matrix considering dispatch factor is:

$$\boldsymbol{C}=-\boldsymbol{Y}\boldsymbol{Q}^{-1}\boldsymbol{R}=\begin{bmatrix}\eta_{\mathrm{Q}}\alpha_{\mathrm{R}}\eta_{\mathrm{WARG}} & \eta_{\mathrm{Q}}\alpha_{\mathrm{Q}} & \eta_{\mathrm{W}}\end{bmatrix}^{T} \tag{44}$$

This result is identical to Eq. (3), which means that our proposed method is equivalent to the method proposed in [18] which considers the dispatch factor in matrix $\boldsymbol{Z}$. The traditional modeling of EH can be viewed as a special case of the method that we propose.

IV. STANDARDIZED MODELING OF ENERGY STORAGE AND INTEGRATED DEMAND RESPONSE

A. Energy Storage

Like Kirchhoff's current law (KCL) in electrical network analysis, Eq. (20) expresses the instantaneous energy balance in each node. It does not hold if energy can be stored in a node and should, therefore, be revised to ensure the validity of the standardized matrix modeling of MES with devices that store energy in any form. There are various kinds of storage in MES such as a battery, compressed air energy storage, the power to gas (P2G) device, thermal storage, and gas storage. Storage devices can be modeled as a two-port converter where the input port models charging and the output port discharging. If we denote by v_g the charging / discharging power of storage device g, the rate of changes of the state of charge of this device is:

$$\Delta E_g=\eta_g v_g \tag{45}$$

where η_g is related to the charging and discharging efficiencies. η_{C} and η_{D} as follows:

$$\eta_g=\begin{cases}\eta_{\mathrm{C}} & v_g>0(\text{charging})\\ 1/\eta_{\mathrm{D}} & v_g\le 0(\text{discharging})\end{cases} \tag{46}$$

Since the port-branch incidence matrix $\boldsymbol{A}_g$ describes the relations between the ports of node g and all the branches. $\boldsymbol{A}_g$ is thus a $K_g\times B$ matrix. To model the state of charge ΔE_g,

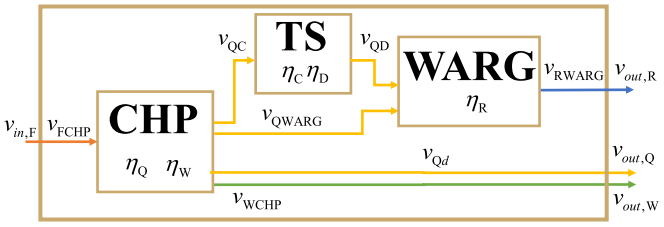

Fig. 3. A CCHP based MES with thermal storage.

we introduce a virtual port and a virtual branch and construct an *augmented port-branch incidence matrix* $\boldsymbol{A}'_g$ of dimension $(K_g+1)\times(B+1)$:

$$\boldsymbol{A}'_g = \begin{bmatrix} \boldsymbol{A}_g & \boldsymbol{0} \\ \boldsymbol{0} & -1 \end{bmatrix} \tag{47}$$

The virtual branch is not a normal branch. It is connected to "the state of charge (SOC)" of the storage. Thus, its flow could be positive (charge) or negative (discharge).

As shown in Fig. 3, let us add thermal storage to the CCHP example. A fraction of the heat produced by the CHP is stored in the thermal storage for use by the water absorption refrigerator group (WARG). The energy flows in the branches are represented by the following vector:

$$\boldsymbol{V} = \left[v_{\mathrm{FCHP}}, v_{\mathrm{QC}}, v_{\mathrm{QWARG}}, v_{\mathrm{QD}}, v_{Qd}, v_{\mathrm{WCHP}}, v_{\mathrm{RWARG}}\right]^T \tag{48}$$

If we number the thermal storage device as node #3, and its charge, discharge, and virtual ports as #1, #2, and #3 respectively, we can form the augmented port-branch incidence matrix:

$$\boldsymbol{A}'_3 = \begin{bmatrix} 0 & 1 & 0 & 0 & 0 & 0 & 0 & 0 \\ 0 & 0 & 0 & -1 & 0 & 0 & 0 & 0 \\ 0 & 0 & 0 & 0 & 0 & 0 & 0 & -1 \end{bmatrix} \tag{49}$$

Considering the energy balance of storage, its converter characteristic matrix is:

$$\boldsymbol{H}_g = \begin{bmatrix} \eta_C & 1/\eta_D & 1 \end{bmatrix} \tag{50}$$

The nodal energy conversion matrix for the storage node can be calculated as follows:

$$\boldsymbol{Z}'_g = \boldsymbol{H}_g \boldsymbol{A}'_g \tag{51}$$

For the example of Fig. 1, the nodal energy conversion matrix of the thermal storage is:

$$\boldsymbol{Z}'_3 = \begin{bmatrix} 0 & \eta_C & 0 & -1/\eta_D & 0 & 0 & 0 & -1 \end{bmatrix} \tag{52}$$

The energy balance equation for the storage node is:

$$\begin{bmatrix} \hat{\boldsymbol{Z}}' & -\boldsymbol{I} \end{bmatrix} \begin{bmatrix} \boldsymbol{V} \\ \Delta \boldsymbol{E} \end{bmatrix} = 0 \tag{53}$$

where $\hat{\boldsymbol{Z}}'$ represents the elements in all $\boldsymbol{Z}'_g$ that correspond to the real branch energy flow in $\boldsymbol{V}$, the $-\boldsymbol{I}$ represent the elements that correspond to the virtual branch $\Delta \boldsymbol{E}$.

Adding Eq. (53) to the original set of energy flow equations for the EH, we get:

$$\begin{bmatrix} \boldsymbol{X} & \boldsymbol{0} \\ \boldsymbol{Y} & \boldsymbol{0} \\ \boldsymbol{Z} & \boldsymbol{0} \\ \hat{\boldsymbol{Z}}' & -\boldsymbol{I} \end{bmatrix} \begin{bmatrix} \boldsymbol{V} \\ \Delta \boldsymbol{E} \end{bmatrix} = \begin{bmatrix} \boldsymbol{V}_{in} \\ \boldsymbol{V}_{out} \\ \boldsymbol{0} \\ \boldsymbol{0} \end{bmatrix} \tag{54}$$

Reorganizing these equations gives:

$$\begin{bmatrix} \boldsymbol{0} & \boldsymbol{0} & \boldsymbol{Y} \\ -\boldsymbol{I} & \boldsymbol{0} & \boldsymbol{X} \\ \boldsymbol{0} & -\boldsymbol{I} & \hat{\boldsymbol{Z}}' \\ \boldsymbol{0} & \boldsymbol{0} & \boldsymbol{Z} \end{bmatrix} \begin{bmatrix} \boldsymbol{V}_{in} \\ \Delta \boldsymbol{E} \\ \boldsymbol{V} \end{bmatrix} = \begin{bmatrix} \boldsymbol{V}_{out} \\ \boldsymbol{0} \\ \boldsymbol{0} \\ \boldsymbol{0} \end{bmatrix} \tag{55}$$

If we define $\boldsymbol{X}' = [\,\boldsymbol{X}^T \quad \hat{\boldsymbol{Z}}'^T\,]^T$ and $\boldsymbol{V}'_{in} = [\,\boldsymbol{V}_{in}^T \quad \Delta \boldsymbol{E}^T\,]^T$, we obtain an expression similar to Eq. (29):

$$\begin{bmatrix} \boldsymbol{0} & \boldsymbol{Y} \\ -\boldsymbol{I} & \boldsymbol{X}' \\ \boldsymbol{0} & \boldsymbol{Z} \end{bmatrix} \begin{bmatrix} \boldsymbol{V}'_{in} \\ \boldsymbol{V} \end{bmatrix} = \begin{bmatrix} \boldsymbol{V}_{out} \\ \boldsymbol{0} \\ \boldsymbol{0} \end{bmatrix} \tag{56}$$

Compared with the basic input incidence matrix $\boldsymbol{X}$, the augmented input incidence matrix has two additional columns and one more row. $\Delta \boldsymbol{E}$ in the $\boldsymbol{V}'_{in}$ introduces one additional column. Therefore adding storage increases the degree of freedom of the EH by two. In the example, one additional degree stems from the dispatch factor of the CHP output and the other from the virtual branch, reflecting the decision of whether to charge or discharge.

Then, we can calculate the energy stored at time t:

$$\boldsymbol{E}(t) = \boldsymbol{E}(t-1) + \Delta \boldsymbol{E}(t) \tag{57}$$

Besides the efficiency constraints described above, constraints on the charge and discharge rates and the SOC must also be considered in operational optimization:

$$0 \le \Delta \boldsymbol{E} \le \Delta \boldsymbol{E}_{\max} \tag{58}$$

$$\boldsymbol{E}_{\min} \le \boldsymbol{E} \le \boldsymbol{E}_{\max}. \tag{59}$$

B. Integrated Demand Response

We have so far assumed that the demand for each type of energy is fixed for each time period. Flexibility in the demand for electricity (i.e., demand response) has been shown to be an effective way to reduce the total cost of operating a power system and the cost to the consumers. Multiple energy systems can extend this concept to integrated demand response, i.e., flexibility in the demand, not only in time but also between various forms of energy. Integrated demand response involves shifting energy use from one form to another. For example, when the electricity price is high, gas can be used for cooking and heating instead of electricity. In an MES, integrated demand response is equivalent to a virtual energy converter connected to the output ports, as shown in Fig. 4.

To model the integrated demand response in this example, we add node D to represent the virtual energy converter, as well as a set of input branches $\boldsymbol{V}_1$ and a set of output branches $\boldsymbol{V}_2$. The input and output incidence matrices must in turn be augmented by adding incidence sub-matrices $\boldsymbol{K}_1$ and $\boldsymbol{K}_2$, which are built in a similar manner as the original input and

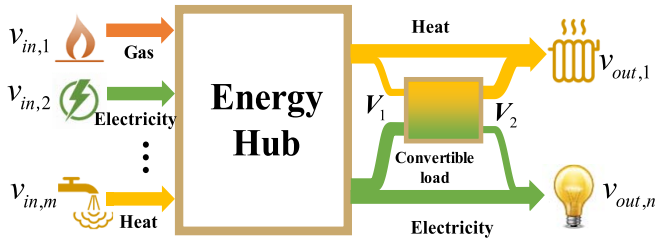

Fig. 4. Energy hub with integrated demand response.

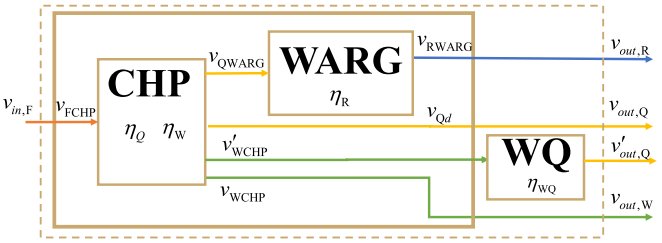

Fig. 5. A CCHP based MES with integrated demand response.

output incidence matrices. The input and output vectors are then defined as follows:

$$\boldsymbol{V}_{in} = \begin{bmatrix} \boldsymbol{P} & \boldsymbol{K}_1 & \boldsymbol{0} \end{bmatrix} \begin{bmatrix} \boldsymbol{V} \\ \boldsymbol{V}_1 \\ \boldsymbol{V}_2 \end{bmatrix} \tag{60}$$

$$\boldsymbol{V}_{out} = \begin{bmatrix} \boldsymbol{Q} & \boldsymbol{0} & \boldsymbol{K}_2 \end{bmatrix} \begin{bmatrix} \boldsymbol{V} \\ \boldsymbol{V}_1 \\ \boldsymbol{V}_2 \end{bmatrix} \tag{61}$$

Fig. 5 adds the integrated demand response to the CCHP example. We assume that on the demand side consumers can choose to use heat pumps for heating instead of the heat provided by the EH. The virtual energy converter WQ (electricity to heat) represents this kind of integrated demand response. We have:

$$\boldsymbol{V}_1 = v'_{\mathrm{WCHP}} \tag{62}$$

$$\boldsymbol{V}_2 = v'_{out,\mathrm{Q}} \tag{63}$$

$$\boldsymbol{K}_1 = \begin{bmatrix} 0 & 0 & 0 \end{bmatrix}^T \tag{64}$$

$$\boldsymbol{K}_2 = \begin{bmatrix} 0 & 1 & 0 \end{bmatrix}^T \tag{65}$$

The port-branch incidence matrices must be augmented to reflect these virtual additions to the EH. For node g, the columns corresponding to original branches are identical to the columns of the original port-branch incidence matrices $\boldsymbol{A}_g$, while the columns corresponding to $\boldsymbol{V}_1$ are denoted $\boldsymbol{A}_{g\mathrm{D}}$. Since the newly added branches $\boldsymbol{V}_2$ are only connected to the output of the virtual node, the columns of the expanded matrices corresponding to $\boldsymbol{V}_2$ are $\boldsymbol{0}$. The augmented port-branch incidence matrices $\boldsymbol{A}'_g$ can be written as follows:

$$\boldsymbol{A}'_g = \begin{bmatrix} \boldsymbol{A}_g & \boldsymbol{A}_{g\mathrm{D}} & \boldsymbol{0} \end{bmatrix} \tag{66}$$

For the virtual node modeling the integrated demand response, the port-branch incidence matrix is:

$$\boldsymbol{A}_D = \begin{bmatrix} \boldsymbol{0} & \boldsymbol{A}_{\mathrm{D1}} & \boldsymbol{A}_{\mathrm{D2}} \end{bmatrix} \tag{67}$$

where $\boldsymbol{A}_{\mathrm{D1}}$ and $\boldsymbol{A}_{\mathrm{D2}}$ correspond to $\boldsymbol{V}_1$ and $\boldsymbol{V}_2$. We can then build the nodal energy conversion matrix for each node:

$$\boldsymbol{Z}''_g = \begin{bmatrix} \boldsymbol{Z}_g & \boldsymbol{H}_g\boldsymbol{A}_{g\mathrm{D}} & \boldsymbol{0} \end{bmatrix} \tag{68}$$

The revised system energy conversion matrix can be written as $[\boldsymbol{Z} \quad \hat{\boldsymbol{Z}}'' \quad \boldsymbol{0}]$, where $\hat{\boldsymbol{Z}}''$ denotes the elements that correspond to $\boldsymbol{H}_g\boldsymbol{A}_{g\mathrm{D}}$ in $\boldsymbol{Z}''_g$.

The nodal energy conversion matrix for the integrated demand response node is:

$$\boldsymbol{Z}_D = \begin{bmatrix} \boldsymbol{0} & \boldsymbol{H}_D\boldsymbol{A}_{\mathrm{D1}} & \boldsymbol{H}_D\boldsymbol{A}_{\mathrm{D2}} \end{bmatrix} \tag{69}$$

where $\boldsymbol{H}_D$ denotes the converter characteristic matrix of the integrated demand response. $\boldsymbol{H}_D$ quantifies the substitution relationship between the types of energy delivered to the consumer.

The comprehensive energy flow equations can then be written as follows:

$$\begin{bmatrix} \boldsymbol{X} & \boldsymbol{K}_1 & \boldsymbol{0} \\ \boldsymbol{Y} & \boldsymbol{0} & \boldsymbol{K}_2 \\ \boldsymbol{Z} & \hat{\boldsymbol{Z}}'' & \boldsymbol{0} \\ \boldsymbol{0} & \boldsymbol{H}_D\boldsymbol{A}_{\mathrm{D1}} & \boldsymbol{H}_D\boldsymbol{A}_{\mathrm{D2}} \end{bmatrix} \begin{bmatrix} \boldsymbol{V} \\ \boldsymbol{V}_1 \\ \boldsymbol{V}_2 \end{bmatrix} = \begin{bmatrix} \boldsymbol{V}_{in} \\ \boldsymbol{V}_{out} \\ \boldsymbol{0} \\ \boldsymbol{0} \end{bmatrix} \tag{70}$$

Reorganizing (70), we get:

$$\begin{bmatrix} \boldsymbol{0} & \boldsymbol{Q} & \boldsymbol{0} & \boldsymbol{K}_2 \\ -\boldsymbol{I} & \boldsymbol{X} & \boldsymbol{K}_1 & \boldsymbol{0} \\ \boldsymbol{0} & \boldsymbol{Z} & \hat{\boldsymbol{Z}}'' & \boldsymbol{0} \\ \boldsymbol{0} & \boldsymbol{0} & \boldsymbol{H}_D\boldsymbol{A}_{\mathrm{D1}} & \boldsymbol{H}_D\boldsymbol{A}_{\mathrm{D2}} \end{bmatrix} \begin{bmatrix} \boldsymbol{V}_{in} \\ \boldsymbol{V} \\ \boldsymbol{V}_1 \\ \boldsymbol{V}_2 \end{bmatrix} = \begin{bmatrix} \boldsymbol{V}_{out} \\ \boldsymbol{0} \\ \boldsymbol{0} \\ \boldsymbol{0} \end{bmatrix} \tag{71}$$

Selecting the energy flows $\boldsymbol{V}_1$ as state variables, we have:

$$\begin{bmatrix} -\boldsymbol{I} & \boldsymbol{K}_1 \\ \boldsymbol{0} & \hat{\boldsymbol{Z}}'' \\ \boldsymbol{0} & \boldsymbol{H}_D\boldsymbol{A}_{\mathrm{D1}} \end{bmatrix} \begin{bmatrix} \boldsymbol{V}_{in} \\ \boldsymbol{V}_1 \end{bmatrix} + \begin{bmatrix} \boldsymbol{X} & \boldsymbol{0} \\ \boldsymbol{Z} & \boldsymbol{0} \\ \boldsymbol{0} & \boldsymbol{H}_D\boldsymbol{A}_{\mathrm{D2}} \end{bmatrix} \begin{bmatrix} \boldsymbol{V} \\ \boldsymbol{V}_2 \end{bmatrix} = \boldsymbol{0} \tag{72}$$

We select $\boldsymbol{V}_1$ as state variables because there are dispatch factors between energy flows in the original branches and the branches connected to the virtual node. If the dimension of $\boldsymbol{V}_1$ is a, and the matrices $[\boldsymbol{X}^T \quad \boldsymbol{Z}^T]^T$ and $\boldsymbol{H}_{\mathrm{D}}\boldsymbol{A}_{\mathrm{D2}}$ have b and c degrees of freedom respectively, the overall degree of freedom of the EH is:

$$f = a + b + c \tag{73}$$

Equation (73) shows that the degree of freedom of the EH considering the integrated demand response has three components: the freedom degree of the original EH, the freedom by the dispatch factors, and the conversion characteristics of the integrated demand response. Note that the degree of freedom of $\boldsymbol{H}_{\mathrm{D}}\boldsymbol{A}_{\mathrm{D2}}$ may be zero or negative. For example, the degree of freedom of WQ in Fig. 3 is zero since the heat output is proportional to its electricity input. For the node with two input ports and one output port, if the two input must be proportional, the degree of freedom is -1.

In the MES shown in Fig. 3, the port-branch incidence submatrices are:

$$\boldsymbol{A}_{g\mathrm{D}} = \begin{bmatrix} 0 & -1 & 0 \end{bmatrix}^T \tag{74}$$

$$\boldsymbol{A}_D = \begin{bmatrix} 0 & 0 & 0 & 0 & 0 & 1 & 0 \\ 0 & 0 & 0 & 0 & 0 & 0 & -1 \end{bmatrix} \tag{75}$$

Assuming that the efficiency of the integrated demand is η_{QW}, the converter characteristic matrix and nodal energy conversion matrix of the virtual node are:

$$\boldsymbol{H}_D = \begin{bmatrix} \eta_{QW} & 1 \end{bmatrix} \tag{76}$$

$$\boldsymbol{Z}_D = \begin{bmatrix} 0 & 0 & 0 & 0 & 0 & \eta_{QW} & -1 \end{bmatrix} \tag{77}$$

Equation (78) gives the comprehensive system of power flow equations. Note that this system is underdetermined.

$$\begin{bmatrix} 1 & 0 & 0 & 0 & 0 & 0 & 0 \\ 0 & 0 & 0 & 0 & 1 & 0 & 0 \\ 0 & 0 & 1 & 0 & 0 & 0 & 1 \\ 0 & 0 & 0 & 1 & 0 & 0 & 0 \\ \eta_{\mathrm{Q}} & -1 & -1 & 0 & 0 & 0 & 0 \\ \eta_{\mathrm{W}} & 0 & 0 & -1 & 0 & -1 & 0 \\ 0 & \eta_{\mathrm{R}} & 0 & 0 & -1 & 0 & 0 \\ 0 & 0 & 0 & 0 & 0 & \eta_{QW} & -1 \end{bmatrix} \begin{bmatrix} v_{\mathrm{FCHP}} \\ v_{\mathrm{QWARG}} \\ v_{\mathrm{Q}d} \\ v_{\mathrm{WCHP}} \\ v_{\mathrm{RWARG}} \\ v'_{\mathrm{WCHP}} \\ v'_{out,\mathrm{Q}} \end{bmatrix} = \begin{bmatrix} v_{in,\mathrm{F}} \\ v_{out,\mathrm{R}} \\ v_{out,\mathrm{Q}} \\ v_{out,\mathrm{W}} \\ 0 \\ 0 \\ 0 \\ 0 \end{bmatrix} \tag{78}$$

Following the degree of freedom analysis developed in Section III, and selecting the heat input of the WARG (v_{QWARG}) and the electricity used for integrated demand response (v'_{WCHP}), as state variables, we have:

$$\boldsymbol{Q}_1 = \begin{bmatrix} 0 & 0 & 0 & 1 & 0 \\ 0 & 1 & 0 & 0 & 1 \\ 0 & 0 & 1 & 0 & 0 \end{bmatrix} \boldsymbol{Q}_2 = \begin{bmatrix} 0 & 0 \\ 0 & 0 \\ 0 & 0 \end{bmatrix}$$

$$\boldsymbol{T}_1 = \begin{bmatrix} 1 & 0 & 0 & 0 & 0 \\ \eta_{\mathrm{Q}} & -1 & 0 & 0 & 0 \\ \eta_{\mathrm{W}} & 0 & -1 & 0 & 0 \\ 0 & 0 & 0 & -1 & 0 \\ 0 & 0 & 0 & 0 & -1 \end{bmatrix} \boldsymbol{T}_2 = \begin{bmatrix} 0 & 0 \\ -1 & 0 \\ 0 & -1 \\ \eta_{\mathrm{R}} & 0 \\ 0 & \eta_{QW} \end{bmatrix}$$

$$\boldsymbol{R} = \begin{bmatrix} -1 & 0 & 0 & 0 & 0 \end{bmatrix}^T \tag{79}$$

The output vector $\boldsymbol{V}_{out}$ is:

$$\begin{aligned} \boldsymbol{V}_{out} &= -\boldsymbol{Y}_1\boldsymbol{Q}_1^{-1}\boldsymbol{R}\boldsymbol{V}_{in} + \left(\boldsymbol{Y}_2 - \boldsymbol{Y}_1\boldsymbol{Q}_1^{-1}\boldsymbol{Q}_2\right)\boldsymbol{V}_2 \\ &= \begin{bmatrix} 0 \\ \eta_Q \\ \eta_{\mathrm{W}} \end{bmatrix} \boldsymbol{V}_{in} + \begin{bmatrix} \eta_{\mathrm{R}} \\ -1 \\ 0 \end{bmatrix} v_{\mathrm{QWARG}} + \begin{bmatrix} 0 \\ \eta_{\mathrm{QW}} \\ -1 \end{bmatrix} v'_{\mathrm{WCHP}} \end{aligned} \tag{80}$$

Compared to the system without integrated demand response, (80) has an extra degree of freedom. In addition to the dispatch factor between v_{QWARG} and v_{QCHP} in the original system, this extra degree of freedom stems from the dispatch factor between v_{WCHP} and the integrated demand response input v'_{WCHP}. The energy conversion characteristics of the integrated demand response do not add freedom to the system because the matrix $\boldsymbol{A}_{\mathrm{D1}}\boldsymbol{G}_D = -1$ is of full rank and therefore contributes zero degrees of freedom.

The proposed method for modeling integrated demand response can be viewed as a general way of adding a new energy converter of any type to an existing EH.

For an MES with storage and demand response, combining Eq. (55) and (71), we get:

$$\begin{bmatrix} \boldsymbol{0} & \boldsymbol{0} & \boldsymbol{Y} & \boldsymbol{0} & \boldsymbol{K}_2 \\ -\boldsymbol{I} & \boldsymbol{0} & \boldsymbol{X} & \boldsymbol{K}_1 & \boldsymbol{0} \\ \boldsymbol{0} & -\boldsymbol{I} & \hat{\boldsymbol{Z}}' & \boldsymbol{0} & \boldsymbol{0} \\ \boldsymbol{0} & \boldsymbol{0} & \boldsymbol{Z} & \hat{\boldsymbol{Z}}'' & \boldsymbol{0} \\ \boldsymbol{0} & \boldsymbol{0} & \boldsymbol{0} & \boldsymbol{H}_{\mathrm{D}}\boldsymbol{A}_{D1} & \boldsymbol{H}_{\mathrm{D}}\boldsymbol{A}_{D2} \end{bmatrix} \begin{bmatrix} \boldsymbol{V}_{in} \\ \Delta\boldsymbol{E} \\ \boldsymbol{V} \\ \boldsymbol{V}_1 \\ \boldsymbol{V}_2 \end{bmatrix} = \begin{bmatrix} \boldsymbol{V}_{out} \\ \boldsymbol{0} \\ \boldsymbol{0} \\ \boldsymbol{0} \\ \boldsymbol{0} \end{bmatrix} \tag{81}$$

If we define several generalized matrices:

$$\begin{aligned} &\tilde{\boldsymbol{Y}} = \begin{bmatrix} \boldsymbol{Y} & \boldsymbol{0} & \boldsymbol{K}_1 \end{bmatrix} \\ &\tilde{\boldsymbol{X}} = \begin{bmatrix} \boldsymbol{X} & \boldsymbol{K}_1 & \boldsymbol{0} \\ \hat{\boldsymbol{Z}}' & \boldsymbol{0} & \boldsymbol{0} \end{bmatrix},\ \tilde{\boldsymbol{Z}} = \begin{bmatrix} \boldsymbol{Z} & \hat{\boldsymbol{Z}}'' & \boldsymbol{0} \\ \boldsymbol{0} & \boldsymbol{H}_{\mathrm{D}}\boldsymbol{A}_{D1} & \boldsymbol{H}_{\mathrm{D}}\boldsymbol{A}_{D2} \end{bmatrix} \\ &\tilde{\boldsymbol{V}}_{in} = \begin{bmatrix} \boldsymbol{V}_{in}^T & \Delta\boldsymbol{E}^T \end{bmatrix}^T,\ \tilde{\boldsymbol{V}} = \begin{bmatrix} \boldsymbol{V}^T & \boldsymbol{V}_1^T & \boldsymbol{V}_2^T \end{bmatrix}^T \end{aligned} \tag{82}$$

Eq. (81) can be reorganized as follows:

$$\begin{bmatrix} \boldsymbol{0} & \tilde{\boldsymbol{Y}} \\ -\boldsymbol{I} & \tilde{\boldsymbol{X}} \\ \boldsymbol{0} & \tilde{\boldsymbol{Z}} \end{bmatrix} \begin{bmatrix} \tilde{\boldsymbol{V}}_{in} \\ \tilde{\boldsymbol{V}} \end{bmatrix} = \begin{bmatrix} \boldsymbol{V}_{out} \\ \boldsymbol{0} \\ \boldsymbol{0} \end{bmatrix}. \tag{83}$$

V. Standardized Data Structure

This section proposes a standardized data structure for EH which supports an automatic procedure for building the coupling matrix of any EH and related computations.

We formulate the data structure of EH analogously to the power system modeling in Matpower [21]. The system matrices, such as the node admittance matrix, can be formed automatically using standardized inputs (such as bus table, generation table, and branch table). Power flow and optimal power flow (OPF) models can then be developed. Following the idea of Matpower, we define a structure with two basic tables for the standardized input for MES information. Let us name this structure ehc (energy hub case) which includes a node table (ehc.node) and branch table (ehc.branch).

For the node table, each row describes a single energy converter in the EH, including:

- A *node ID* for each energy converter, numbered in order starting from 1. Especially, the inputs and outputs of EH are special nodes and numbered -1 and 0 respectively.
- The *node type* is used to identify the type and operating status of each energy converter. For example, 1 for WARG; 2 for CHP unit in extraction condensing operation and 3 for the same in back pressure operation; 4 for the P2G device and so on.
- The node parameters provide information specific to the energy conversion characteristics of an energy converter. For example, the efficiencies of converting gas to electricity and heat in a CHP unit. Other parameters of energy converters, such as the minimum capacity or ramp rate, can also be included when modeling the operating constraints of the EH. However, the coupling matrix modeling only requires the energy conversion characteristics. The number of parameters depends on the type of node.

For the branch table, each row describes one energy flow in the EH, including.

TABLE II
NODE TABLE OF THE EH IN FIG. 1

No.	Node	Node Type	Parameters	
-1	Input	-1	0	0
0	Output	0	0	0
1	CHP	3	η_{Q}	η_{W}
2	WARG	1	η_{WARG}	0

TABLE III
BRANCH TABLE OF THE EH IN FIG. 1

No.	Branch	Branch Type	Source	Sink	Parameters
1	v_{FCHP}	4	-1	1	0
2	v_{QWARG}	3	1	2	0
3	v_{QCHP}	3	1	0	300
4	v_{WCHP}	1	1	0	0
5	v_{RWARG}	2	2	0	0

- A *branch ID* of each energy flow in the EH, numbered from 1.
- The *branch type* identifies the type of each energy flow. For example, the electricity, heat, cooling, and gas flows are numbered as 1, 2, 3, and 4 respectively.
- The ID of the *source node* of the branch.
- The ID of the *sink node* of the branch.
- The *branch parameters* provide information specific to the branch, such as its capacity.

The converter characteristic matrix $\boldsymbol{H}_g$ for each converter can be obtained from the node table. The port-branch incidence matrix $\boldsymbol{A}_g$, input incidence matrix $\boldsymbol{X}$, and output incidence matrix $\boldsymbol{Y}$ can be formed based on the branch table. We can further define other tables to provide more information such as the operating costs of the converters and the energy demands at different times for applications such as energy flow calculations and optimization. Taking the EH shown in Fig. 2 as example, the node table and branch table are shown as Table II and Table III. The column "parameters" of Table III gives the capacity of each branch, where 0 means the branch has no capacity limit. For example, 300 in the third column of Table III means that the energy flow capacity of the third branch is 300 kW.

VI. CASE STUDY

The section illustrates the standardized matrix modeling process of a modified tri-generation system with storage and integrated demand response and its application to operational optimization.

A. System Description

Figure 6 illustrates a complex tri-generation system modified from the system proposed in [18], which consists of a CHP unit in back pressure operation mode, an auxiliary boiler (AB), a compression electric refrigerator group (CERG), a WARG, a thermal storage (TS), and a electricity to heat

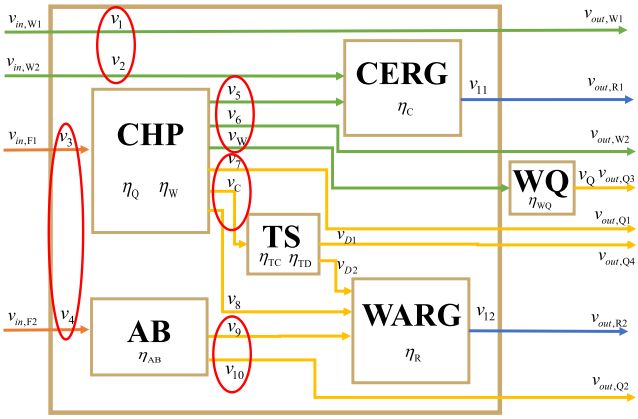

Fig. 6. A complex tri-generation system with thermal storage and integrated demand response.

integrated demand response (WQ). The energy inputs are electricity and gas, while the outputs include cooling, heat and electricity. TS is connected to the CHP on its input side and to the WARG and the EH output. We also insert a WQ at the output of the CHP unit which is able to shift from electricity to heat. Table I lists the parameters of the energy converters of this system.

B. Standardized Matrix Formulation

Without consideration of TS and WQ, there are 12 branches and 4 nodes. The CHP, AB, CERG and WARG are numbered nodes 1, 2, 3, and 4, respectively. The parameters of each energy converter and the name of each branch are shown in Fig. 4. The port-branch incidence matrix for each node are:

$$\begin{aligned}
\boldsymbol{A}_1 &= \begin{bmatrix} 0 & 0 & 1 & 0 & 0 & 0 & 0 & 0 & 0 & 0 & 0 & 0 \\ 0 & 0 & 0 & 0 & -1 & -1 & 0 & 0 & 0 & 0 & 0 & 0 \\ 0 & 0 & 0 & 0 & 0 & 0 & -1 & -1 & 0 & 0 & 0 & 0 \end{bmatrix} \\
\boldsymbol{A}_2 &= \begin{bmatrix} 0 & 0 & 0 & 1 & 0 & 0 & 0 & 0 & 0 & 0 & 0 & 0 \\ 0 & 0 & 0 & 0 & 0 & 0 & 0 & 0 & -1 & -1 & 0 & 0 \end{bmatrix} \\
\boldsymbol{A}_3 &= \begin{bmatrix} 0 & 1 & 0 & 0 & 1 & 0 & 0 & 0 & 0 & 0 & 0 & 0 \\ 0 & 0 & 0 & 0 & 0 & 0 & 0 & 0 & 0 & 0 & -1 & 0 \end{bmatrix} \\
\boldsymbol{A}_4 &= \begin{bmatrix} 0 & 0 & 0 & 0 & 0 & 0 & 0 & 1 & 1 & 0 & 0 & 0 \\ 0 & 0 & 0 & 0 & 0 & 0 & 0 & 0 & 0 & 0 & 0 & -1 \end{bmatrix}
\end{aligned} \tag{84}$$

The converter characteristic matrices are:

$$\begin{aligned}
\boldsymbol{H}_1 &= \begin{bmatrix} \eta_{\mathrm{Q}} & 1 & 0 \\ \eta_{\mathrm{W}} & 0 & 1 \end{bmatrix} \\
\boldsymbol{H}_2 &= \begin{bmatrix} \eta_{\mathrm{AB}} & 1 \end{bmatrix} \\
\boldsymbol{H}_3 &= \begin{bmatrix} \eta_{\mathrm{C}} & 1 \end{bmatrix} \\
\boldsymbol{H}_4 &= \begin{bmatrix} \eta_{\mathrm{R}} & 1 \end{bmatrix}
\end{aligned} \tag{85}$$

The input incidence matrix $\boldsymbol{X}$ and output incidence matrix $\boldsymbol{Y}$ are:

$$\begin{aligned}
\boldsymbol{X} &= \begin{bmatrix} 1 & 1 & 0 & 0 & 0 & 0 & 0 & 0 & 0 & 0 & 0 & 0 \\ 0 & 0 & 1 & 1 & 0 & 0 & 0 & 0 & 0 & 0 & 0 & 0 \end{bmatrix} \\
\boldsymbol{Y} &= \begin{bmatrix} 1 & 0 & 0 & 0 & 0 & 1 & 0 & 0 & 0 & 0 & 0 & 0 \\ 0 & 0 & 0 & 0 & 0 & 0 & 0 & 0 & 0 & 0 & 1 & 1 \\ 0 & 0 & 0 & 0 & 0 & 0 & 1 & 0 & 0 & 1 & 0 & 0 \end{bmatrix}
\end{aligned} \tag{86}$$

The system energy conversion matrix without TS and WQ is:

$$\boldsymbol{Z}=\begin{bmatrix} 0 & 0 & \eta_Q & 0 & -1 & -1 & 0 & 0 & 0 & 0 & 0 & 0 \\ 0 & 0 & \eta_W & 0 & 0 & 0 & -1 & -1 & 0 & 0 & 0 & 0 \\ 0 & 0 & 0 & \eta_{AB} & 0 & 0 & 0 & 0 & -1 & -1 & 0 & 0 \\ 0 & \eta_C & 0 & 0 & \eta_C & 0 & 0 & 0 & 0 & 0 & -1 & 0 \\ 0 & 0 & 0 & 0 & 0 & 0 & 0 & \eta_R & \eta_R & 0 & 0 & -1 \end{bmatrix} \tag{87}$$

To add the TS and WQ into the original tri-generation system proposed in [18], the port-branch incidence matrix and input/output incidence matrix should be revised accordingly.

Especially, the matrices related to TS can be formed as Eq. (88) according to Eqs. (47) and (51):

$$\hat{\boldsymbol{Z}}'=\begin{bmatrix} 0\,0\,0\,0\,0\,0\,0\,0\,0\,0\,0\,0\,\eta_{TC} & -1/\eta_{TD} & -1/\eta_{TD} \end{bmatrix} \tag{88}$$

The matrices related to WQ can be formed as Eq. (89) according to Eqs. (66) to (69):

$$\hat{\boldsymbol{Z}}''=\begin{bmatrix} -1 & 0 & 0 & 0 & 0 \end{bmatrix}^T \tag{89}$$

Equation (94), as shown at the bottom of the next page, shows the reorganized comprehensive energy flow equations. The matrix is divided into 5×5 blocks which correspond to Eq. (81). Rows 1-3 refer to the correspondence between branch energy flows and output energy. Rows 4-5 refer to the correspondence between branch energy flows and input energy. Row 6 describes the thermal storage. Rows 7-11 are similar to the original comprehensive energy flow equations without TS and WQ. The last row corresponds to the integrated demand response.

C. Degree of Freedom Analysis

For the original tri-generation system without TS and WQ, if we select the power flows, v_2, v_3, v_5, v_7, and v_9, as state variables, the coupling matrix can then be calculated based on the results of $\boldsymbol{Z}$ shown in (87):

$$\boldsymbol{V}_{out}=\begin{bmatrix} 1 & 0 & -1 & \eta_{\mathrm{W}} & -1 & 0 & 0 \\ 0 & 0 & \eta_C & \eta_{\mathrm{Q}}\eta_{\mathrm{R}} & \eta_{\mathrm{C}} & -\eta_{\mathrm{R}} & \eta_{\mathrm{R}} \\ 0 & \eta_{\mathrm{AB}} & 0 & -\eta_{\mathrm{B}} & 0 & 1 & -1 \end{bmatrix}\begin{bmatrix} v_{in,1} \\ v_{in,2} \\ v_2 \\ v_3 \\ v_5 \\ v_7 \\ v_9 \end{bmatrix} \tag{90}$$

From (86) and (87), we conclude that $\boldsymbol{Q}$ is a 7×12 matrix. The degree of freedom is thus five, which corresponds to the five dispatch factors highlighted by red circles in Fig. 4. The number of energy conversion equations (θ) is equal to the total number of output ports of all of the nodes (λ), because the energy conversion does not contribute any degree of freedom.

When the TS and WQ are added to the original tri-generation system, the matrix $\boldsymbol{Q}$ becomes a 12×20 matrix. The revised comprehensive energy flow equations thus have nine degrees of freedom. Of these four extra degrees of freedom, one arises from the flexibility introduced by integrated demand response between heat and electricity, one from the charging/discharging flexibility of the thermal storage, and the other two from the dispatch flexibility of the output of the thermal storage (v_{D1} and v_{D2}).

TABLE IV
PARAMETERS OF THE ENERGY CONVERTERS IN FIG. 6

Converter	Capacity(kW)	Efficiency
CHP	400(gas) 120(electricity) 160(thermal)	η_{W} =0.3, η_{Q} =0.4
AB	400	η_{AB} =0.8
CERG	300	η_{C} =3
WARG	300	η_{R} =0.7
TS	1000*	η_{TC} =0.95, η_{TD} =0.95
WQ	100	η_{WQ} =2

* The capacity of TS denotes the energy capacity (kWh)

D. Multi-Periods Optimal Operation for EH

In this tri-generation system, the consumers' hourly summer demands for electricity, heat and cooling and the hourly price of electricity varies are the same as in [18], while the price of gas is 40 Euro/MWh and is constant over the day.

The optimal energy flow of a single EH determines how the energy flow should be dispatched among different converters to minimize the cost or maximize the profit of the whole system over a given time horizon. The objective is to minimize the total cost of energy over the day:

$$\min \sum_{t=1}^{T}\sum_{m=1}^{M} f_{m,t}v_{in,m,t} \tag{91}$$

where m and t are the indices for the type of energy input of the EH and the time period; M, and T denote the total number of types of energy input and the total number of time periods; $v_{in,m,t}$ and $f_{m,t}$ denote the m-th type of input energy and the corresponding price at the time period t.

Each energy converter or storage must operate within its capacity:

$$\boldsymbol{0} \le \boldsymbol{A}_{g,t}\boldsymbol{V}_t \le \boldsymbol{C}_{\max g} \quad \forall g,t \tag{92}$$

where $\boldsymbol{A}_{g,t}\boldsymbol{V}_t$ denotes the energy flow of the ports of the g-th energy converter; $\boldsymbol{C}_{\max g}$ the capacity of the g-th energy converter or the maximum charging and discharging rate of the g-th energy storage device. Table IV shows the capacity constraints on the energy converters.

The energy flows in the EH should satisfy the comprehensive of energy flow equations as shown in Eq. (94), at the bottom of the next page. The constraints for energy storage can refer to Eqs. (57) to (59).

Finally, the proposed optimal operation model can be summarized as follows:

$$\begin{aligned} &OF: Eq.(91) \\ &s.t.\ Eqs.\ (92), (94), (57)-(59) \end{aligned} \tag{93}$$

Four cases are considered: Case 1: considering both thermal storage (TS) and integrated demand response (WQ); Case 2: considering only WQ; Case 3: considering only TS;

TABLE V
COMPARISON OF PERFORMANCE BETWEEN LINEAR AND NONLINEAR METHODS

Case	Optimal Value (Euro)		Computation Time (s)	
	Linear	Nonlinear	Linear	Nonlinear
#1	365.24	369.74	0.0598	105.3667
#2	369.32	378.55	0.0588	42.7079
#3	377.24	378.73	0.0557	104.9060
#4	377.90	378.59	0.0528	22.7543

Case 4: considering neither TS nor WQ. The four optimization models are implemented in MATLAB with YALMIP on a PC with Intel Core i7 2.60 GHz CPU and 8 GB RAM [22]. The linear model is solved using CPLEX. The nonlinear model is solved using fmincon with the SQP method. The maximum number of iterations is set at 3000. The result obtained with the linear model of Case 4 provide an initial solution for the nonlinear cases.

Table V summarizes the optimal operating costs and computing times for the linear and nonlinear models for these four cases. Since the choice of state variables makes our proposed model linear and convex, the solutions obtained with our proposed method are globally optimum. Solving this convex problem also requires less computing time. The introduction of TS and WQ reduces the total cost by about 3.47%. Experiments with nonlinear optimization problems show that their solutions are time-consuming. When TS is not considered (Case 2 and Case 4), local optimal can be reached. Cases 1 and 3, which consider TS, exceed the maximum iterations because TS introduces complex time coupling constraints. Optimality cannot be guaranteed with nonlinear models.

Fig. 7 shows the operating states of each energy converter in the EH over a 24-hour period obtained with the proposed linear model. The electricity demand is provided by the CHP when the price of electricity is high. The heat is supplied mainly by the CHP unit. When the CHP reaches its capacity, the integrated demand response WQ is used to meet the heat demand. Because of the high efficiency of the CERG, cooling relies mainly on electricity. The WARG is used as a supplemental source when the CERG reaches its capacity limit. The thermal storage and the integrated demand response provide flexibility to the EH and reduce the total cost.

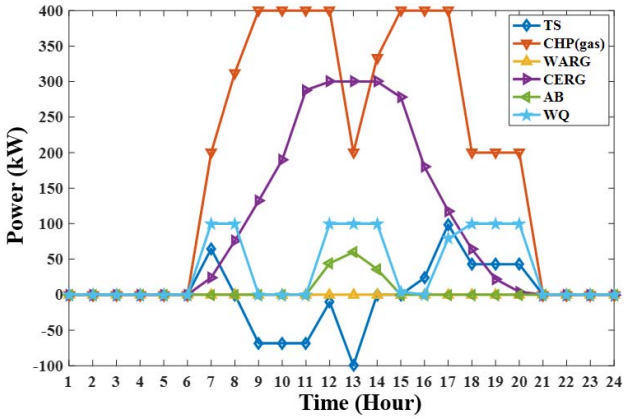

Fig. 7. Operating states of the energy converters in the EH obtained by linear model.

Fig. 8 shows the operating states of each energy converters in the EH over a 24-hour period obtained by dispatch factors based nonlinear model. It can be seen that the operating states of the energy converters are similar to that obtained by linear model. However, the operation of TS is not identical showing that nonlinear model cannot guarantee optimal solution with more complex constraints. The proposed linear model facilitates an efficient operation optimization of EH that guarantees the optimality.

$$\left[\begin{array}{ccc|cccccccccccccccc|cc}
0 & 0 & 0 & 1 & 0 & 0 & 0 & 0 & 1 & 0 & 0 & 0 & 0 & 0 & 0 & 0 & 0 & 0 & 0 & 0 \\
0 & 0 & 0 & 0 & 0 & 0 & 0 & 0 & 0 & 0 & 0 & 0 & 0 & 1 & 1 & 0 & 0 & 0 & 0 & 0 \\
0 & 0 & 0 & 0 & 0 & 0 & 0 & 0 & 0 & 1 & 0 & 0 & 1 & 0 & 0 & 0 & 1 & 0 & 0 & 1 \\
\hdashline
-1 & 0 & 0 & 1 & 1 & 0 & 0 & 0 & 0 & 0 & 0 & 0 & 0 & 0 & 0 & 0 & 0 & 0 & 0 & 0 \\
0 & -1 & 0 & 0 & 0 & 1 & 1 & 0 & 0 & 0 & 0 & 0 & 0 & 0 & 0 & 0 & 0 & 0 & 0 & 0 \\
\hdashline
0 & 0 & -1 & 0 & 0 & 0 & 0 & 0 & 0 & 0 & 0 & 0 & 0 & 0 & 0 & η_{TC} & $-1/\eta_{TD}$ & $-1/\eta_{TD}$ & 0 & 0 \\
\hdashline
0 & 0 & 0 & 0 & 0 & η_Q & 0 & -1 & -1 & 0 & 0 & 0 & 0 & 0 & 0 & 0 & 0 & 0 & -1 & 0 \\
0 & 0 & 0 & 0 & 0 & η_W & 0 & 0 & 0 & -1 & -1 & 0 & 0 & 0 & 0 & -1 & 0 & 0 & 0 & 0 \\
0 & 0 & 0 & 0 & 0 & 0 & η_{AB} & 0 & 0 & 0 & 0 & -1 & -1 & 0 & 0 & 0 & 0 & 0 & 0 & 0 \\
0 & 0 & 0 & 0 & η_C & 0 & 0 & η_C & 0 & 0 & 0 & 0 & 0 & -1 & 0 & 0 & 0 & 0 & 0 & 0 \\
0 & 0 & 0 & 0 & 0 & 0 & 0 & 0 & 0 & 0 & η_R & η_R & 0 & 0 & -1 & 0 & 0 & η_R & 0 & 0 \\
\hdashline
0 & 0 & 0 & 0 & 0 & 0 & 0 & 0 & 0 & 0 & 0 & 0 & 0 & 0 & 0 & 0 & 0 & 0 & η_{WQ} & -1
\end{array}\right]
\left[\begin{array}{c}
v_{in,W} \\ v_{in,F} \\ \Delta E \\ \hdashline
v_1 \\ v_2 \\ v_3 \\ v_4 \\ v_5 \\ v_6 \\ v_7 \\ v_8 \\ v_9 \\ v_{10} \\ v_{11} \\ v_{12} \\ v_C \\ \hdashline
v_{D1} \\ v_{D2} \\ \hdashline
v_W \\ \hdashline
v_Q
\end{array}\right]
=
\left[\begin{array}{c}
v_{out,W} \\ v_{out,R} \\ v_{out,Q} \\ \hdashline
0 \\ 0 \\ 0 \\ 0 \\ 0 \\ 0 \\ 0 \\ 0 \\ 0 \\ 0 \\ 0 \\ 0
\end{array}\right] \tag{94}$$

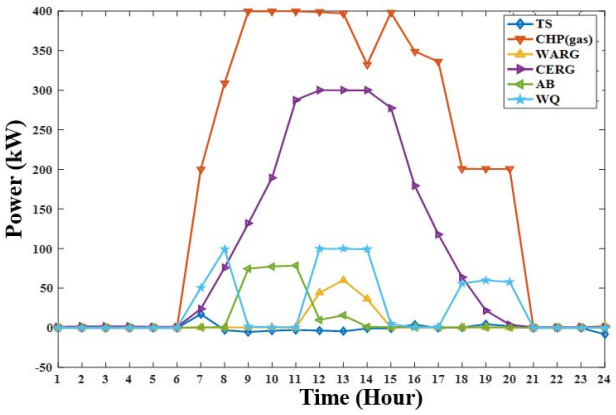

Fig. 8. Operating states of the energy converters in the EH obtained by nonlinear model.

It should be noted that the proposed modeling method is able to formulate the optimal operation of EH into a linear programming (LP) problem. Since large-scale LP problem can be solved by existed software with high computation efficiency, our proposed method is applicable for large-scale system and obtain global optimal operation decision.

VII. Conclusion

This paper proposes a standardized matrix modeling method for MES based on the concept of EH. This method leads to a compact formulation of the characteristics of the energy converters and their connections. A generalized coupling matrix can then be obtained by Gaussian elimination. This model and analysis framework are highly amenable to computer implementation and will thus greatly facilitate the modeling, simulation, and optimization of complex MES. The proposed method can reduce the nonlinearity of the optimization model of EH.

Future works include the standardized optimal operation and planning model for MES and the handling of nonlinear constraints from energy interconnectors and non-constant efficiencies of energy converters.

References

[1] T. Krause, G. Andersson, K. Fröhlich, and A. Vaccaro, "Multiple-energy carriers: Modeling of production, delivery, and consumption," *Proc. IEEE*, vol. 99, no. 1, pp. 15–27, Jan. 2011.

[2] M. Geidl, "Integrated modeling and optimization of multi-carrier energy systems," Ph.D. dissertation, Eidgenössische Technische Hochschule Zürich, Zürich, Switzerland, 2007.

[3] M. Geidl *et al.*, "Energy hubs for the future," *IEEE Power Energy Mag.*, vol. 5, no. 1, pp. 24–30, Jan./Feb. 2007.

[4] Y. Wang, N. Zhang, and C. Q. Kang, "Review and prospect of optimal planning and operation of energy hub in Energy Internet," *China Soc. Elect. Eng.*, vol. 35, no. 22, pp. 5669–5681, 2015.

[5] P. Ahčin and M. Šikić, "Simulating demand response and energy storage in energy distribution systems," in *Proc. Int. Conf. Power Syst. Technol. (POWERCON)*, Hangzhou, China, 2010, pp. 1–7.

[6] Y. Wang *et al.*, "Load profiling and its application to demand response: A review," *Tsinghua Sci. Technol.*, vol. 20, no. 2, pp. 117–129, Apr. 2015.

[7] X. Zhang, G. G. Karady, and S. T. Ariaratnam, "Optimal allocation of CHP-based distributed generation on urban energy distribution networks," *IEEE Trans. Sustain. Energy*, vol. 5, no. 1, pp. 246–253, Jan. 2014.

[8] X. Xu, M. Bishop, D. G. Oikarinen, and C. Hao, "Application and modeling of battery energy storage in power systems," *CSEE J. Power Energy Syst.*, vol. 2, no. 3, pp. 82–90, Sep. 2016.

[9] M. D. Galus and G. Andersson, "Power system considerations of plug-in hybrid electric vehicles based on a multi energy carrier model," in *Proc. IEEE Power Energy Soc. Gen. Meeting*, Calgary, AB, Canada, 2009, pp. 1–8.

[10] Y. Cheng and C. Zhang, "Configuration and operation combined optimization for EV battery swapping station considering PV consumption bundling," *Protect. Control Mod. Power Syst.*, vol. 2, no. 1, p. 26, 2017.

[11] M. Schulze, L. Friedrich, and M. Gautschi, "Modeling and optimization of renewables: Applying the energy hub approach," in *Proc. IEEE Int. Conf. Sustain. Energy Technol.*, Singapore, 2008, pp. 83–88.

[12] A. Sheikhi, M. Rayati, S. Bahrami, and A. M. Ranjbar, "Integrated demand side management game in smart energy hubs," *IEEE Trans. Smart Grid*, vol. 6, no. 2, pp. 675–683, Mar. 2015.

[13] H. A. Thanhtung, Y. Zhang, V. V. Thang, and J. Huang, "Energy hub modeling to minimize residential energy costs considering solar energy and BESS," *J. Mod. Power Syst. Clean Energy*, vol. 5, no. 3, pp. 389–399, 2017.

[14] A. Piacentino, C. Barbaro, F. Cardona, R. Gallea, and E. Cardona, "A comprehensive tool for efficient design and operation of polygeneration-based energy μgrids serving a cluster of buildings. Part I: Description of the method," *Appl. Energy*, vol. 111, pp. 1204–1221, Nov. 2013.

[15] C. Shao, X. Wang, M. Shahidehpour, X. Wang, and B. Wang, "An MILP-based optimal power flow in multicarrier energy systems," *IEEE Trans. Sustain. Energy*, vol. 8, no. 1, pp. 239–248, Jan. 2017.

[16] S. Bahrami and F. Safe, "A financial approach to evaluate an optimized combined cooling, heat and power system," *Energy Power Eng.*, vol. 5, no. 5, pp. 352–362, 2013.

[17] E. A. M. Ceseña, T. Capuder, and P. Mancarella, "Flexible distributed multienergy generation system expansion planning under uncertainty," *IEEE Trans. Smart Grid*, vol. 7, no. 1, pp. 348–357, Jan. 2016.

[18] G. Chicco and P. Mancarella, "Matrix modelling of small-scale trigeneration systems and application to operational optimization," *Energy*, vol. 34, no. 3, pp. 261–273, 2009.

[19] M. R. Almassalkhi and A. Towle, "Enabling city-scale multi-energy optimal dispatch with energy hubs," in *Proc. IEEE Power Syst. Comput. Conf. (PSCC)*, Genoa, Italy, 2016, pp. 1–7.

[20] R. Merris, *Graph Theory*. New York, NY, USA: Wiley, 2000.

[21] R. D. Zimmerman, C. E. Murillo-Sanchez, and R. J. Thomas, "MATPOWER: Steady-state operations, planning, and analysis tools for power systems research and education," *IEEE Trans. Power Syst.*, vol. 26, no. 1, pp. 12–19, Feb. 2011.

[22] J. Lofberg, "YALMIP: A toolbox for modeling and optimization in MATLAB," in *Proc. CACSD Conf.*, New Orleans, LA, USA, 2004, pp. 284–289.

Yi Wang (S'14) received the B.S. degree from the Department of Electrical Engineering, Huazhong University of Science and Technology, Wuhan, China, in 2014.

He is currently pursuing the Ph.D. degree with Tsinghua University. He is also a visiting student researcher with the University of Washington, Seattle, WA, USA. His research interests include data analytics in smart grid and multiple energy systems.

Ning Zhang (S'10–M'12) received the B.S. and Ph.D. degrees from the Electrical Engineering Department, Tsinghua University, China, in 2007 and 2012, respectively.

He is currently an Assistant Professor with Tsinghua University. His research interests include multiple energy system integration, renewable energy, and power system planning and operation.

Chongqing Kang (M'01–SM'08–F'17) received the Ph.D. degree from the Department of Electrical Engineering, Tsinghua University, Beijing, China, in 1997.

He is currently a Professor with Tsinghua University. His research interests include power system planning, power system operation, renewable energy, low carbon electricity technology, and load forecasting.

Daniel S. Kirschen (M'86–SM'91–F'07) received the degree in electrical and mechanical engineering from the Universite Libre de Bruxelles, Brussels, Belgium, in 1979 and the M.Sc. and Ph.D. degrees from the University of Wisconsin, Madison, WI, USA, in 1980 and 1985, respectively.

He is currently a Close Professor of electrical engineering with the University of Washington, Seattle, WA, USA. His research interests include smart grids, integration of renewable energy sources in the grid, power system economics, and power system security.

Jingwei Yang (S'15) received the B.S. degree from the Electrical Engineering Department, Tsinghua University, China, in 2015.

He is currently pursuing the Ph.D. degree with Tsinghua University. His research interests include optimal power flow, renewable energy, and multiple energy system integration.

Qing Xia (M'01–SM'08) received the Ph.D. degree from the Department of Electrical Engineering, Tsinghua University, Beijing, China, in 1989.

He is currently a Professor with Tsinghua University. His research interests include electricity markets, generation scheduling optimization, and power system planning.